Expression of inversin and DVL-1 in the liver of yotari (Dab1-/-) and wild-type mice

Preid Galešić, Vanessa Elena

Download date / Datum preuzimanja: **2025-04-03**

SVEUČILIŠTE U SPLITU
MEDICINSKI FAKULTET
UNIVERSITAS STUDIOURUM SPALATENSIS
FACULTAS MEDICA

Repository / Repozitorij:

MEFST Repository

zir.nsk.hr

UNIVERSITY OF SPLIT

dabar
DIGITALNI AKADEMSKI ARHIVI I REPOZITORIJI

UNIVERSITY OF SPLIT

SCHOOL OF MEDICINE

Vanessa Elena Preid Galešić

EXPRESSION OF INVERSIN AND DVL-1 IN THE LIVER OF *YOTARI* (*DAB1*$^{-/-}$) AND WILD-TYPE MICE

Diploma Thesis

Academic year:

2023/2024

Mentor:

Prof. Katarina Vukojević, MD, PhD

Split, July 2024

Table of Contents

LIST OF ABBREVIATIONS

yot - yotari mice

HSC - hepatic stellate cells

TGFB - transforming growth factor beta

FGF - fibroblast growth factor

Wnt - wingless-related integration site

BMP - bone morphogenetic proteins

RA - retinoic acid

AFP - alpha fetoprotein

HNF4A - heptatocyte nuclear factor 4 alpha

HGF - hepatocyte growth factor

IP3R1 - inositol 1,4,5-trisphosphate receptors

Dab1 *-disabled 1*

FZD - Frizzled

CK1 - Casein kinase 1

GSK3B - Glycogen Synthase Kinase 3 Beta

Invs - Inversin

DVL - Dishevelled

APC - Adenomatous polyposis coli

TCF - T-cell factor

LEF - lymphoid enhancer factor

CBP)/p300 - CREB-binding protein

BCL9 - B-cell CLL/lymphoma protein 9

PLC - phospholipase C

LRP - Lipoprotein receptor-related protein

SMO – Smoothened protein

PCP – planar cell polarity

PTK7 – Protein tyrosine kinase 7

MUSK – Muscle-specific kinase

RYK – Related to receptor tyrosine kinase¸

Vangl2 – VANGL planar cell polarity protein 2

Celsr1 – Cadherin EGF LAG seven-pass G-type receptor 1

DAAM – Dyl-associated activator of morphogenesis

CapZip – CapZ-interacting protein

ROCK – Rho associated protein kinase

DIA1 – Diaphanous-related formin-1

RhoA – Ras homolog family member A

MRLC – Myosin regulatory light chain

Src – Proto-oncogene tyrosine-protein kinase Src

Fyn – Proto-oncogene tyrosine-protein kinase Fyn

ApoER2 – apolipoprotein E receptor 2

VLDLR - very-low-density-lipoprotein receptor

SH2 – Src Homology 2 domain

Crk/C3G/Rap1 -

VEGF - Vascular endothelial growth factor

VEGFR2 – VEGF receptor 2

EGFR – Epidermal growth factor receptor

EGF – Epidermal growth factor

PKD – polycystic kidney disease

DEP – Dishevelled, Egl-10 and Pleckstrin domain

PDZ – postsynaptic density protein (PSD95), Drosophila disc large tumor suppressor (DlgA), and zonula occludens-1 protein

E.13.5 – Embryonic day 13.5

E15.5 – Embryonic day 15.5

PBS – phosphate buffer saline

PFA – paraformaldehyde

H&E – Hematoxylin & Eosin

DAPI – 4′,6-diamidino-2-phenylindole

SD – Standard Deviation

NF-kB – Nuclear factor kappa-light-chain-enhancer of activated B cells

TNF-a – Tumor necrosis factor alpha

IL-6 – Interleukin 6

HCC – Hepatocellular Cancer

CSC – Cancer stem cell

1. INTRODUCTION

1.1. The liver

1.1.1. Anatomy of Liver

The quadrate, caudate, left, and right anatomical lobes make up the liver. The quadrate lobe is located between the left and right lobe on the inferior surface of the right lobe. The majority of the abdomen's right upper quadrant, which is inferior to the diaphragm, is occupied by the liver. It is mostly intraperitoneal from the right costal border to the fifth intercostal space in the midclavicular line. The superior posterior portion of the liver has a bare area where the inferior vena cava and diaphragm are situated. At the margin of the exposed area that forms the coronary ligament, the diaphragm and visceral peritoneum—which covers the remaining section of the liver—come together. The inferior liver is closely associated with the right kidney and gallbladder. Another notable ligament is the Falciform ligament, which separates the liver into anatomic left and right along the anterior section. The liver's free-form edge of the falciform ligament is home to the round ligament, a relic of the embryonic umbilical vein. The caudate lobe is divided medially, posteriorly, and anteriorly, respectively, by the *ligamentum venosum*, inferior *vena cava*, and *porta hepatis*. The *ligamentum venosum* is the remaining portion of the embryonic *ductus venosus*. Located anterior to the *porta hepatis* and lateral to the liver's round ligament, the quadrate lobe is closely associated with the gallbladder. The eight functional divisions of the liver, which are divided according to the blood supply, do not correspond with these anatomic lobes (1).

1.1.2. Histology of Liver

1.1.2.1. Stroma

The liver's histological structure is polygonal, characterized by portal tracts that circumscribe a central vein. This intricate design forms approximately 1 million hepatic microscopic lobules (2). The liver's stroma is composed of connective tissue interwoven with blood vessels, lymphatics, and various cell types, including hepatic stellate cells (HSCs), Kupffer cells, and endothelial cells. The organ's framework is formed by a network of reticular fibers and collagen within the connective tissue. Collagen provides tensile strength, while reticular fibers support the architecture of the liver sinusoids. Blood and lymphatic vessels contribute to the liver's structure, maintaining its blood supply and supporting its physiological functions.

Hepatic stellate cells (HSCs) are pericyte-like cells located between sinusoidal endothelial cells and hepatocytes within the space of Disse. These cells play a crucial role in liver regeneration and fibrosis. In response to liver injury, HSCs become activated, proliferate, and produce extracellular matrix components such as collagen, which contribute to the development of fibrosis. Kupffer cells, specialized macrophages also known as stellate sinusoidal macrophages or Kupffer-Browicz cells, reside in the liver's sinusoids. They are pivotal in tissue homeostasis and immune defense, performing phagocytosis of pathogens, foreign particles, and damaged cells. Endothelial cells lining the sinusoids regulate the exchange of metabolites between blood and hepatocytes and are involved in hepatic angiogenesis and the release of inflammation-related factors (3–5)

1.1.2.2. Hepatic Lobules

The functional unit of the liver is the hepatic lobule. The lobule is arranged in a hexagonal shape around the central vein. The vertex of these hexagons is the portal triad made of the hepatic artery, bile ducts and portal vein. Unlike the capillaries in other body parts, hepatic capillaries do not form tight junctions, allowing blood to be filtered between hepatocytes for the liver's metabolic function. The blood transverses from the hepatic artery as oxygen-rich blood, mixes with nutrient-filled blood flowing through the lobules and exits through the portal. Through the lobules, gradient differences of oxygen, nutrients and waste products contribute to the uptake and elimination of molecules in the blood. The specific functions and gradients are sectioned off into zones based on the location and function of the hepatocytes. This is called metabolic zonation, which is partitioned into three zones with different gene expressions and functions of the hepatocytes. Pathological damage to the liver or any loss of function can lead to hepatocytes changing their gene expression and changing their metabolic zone function (2). The lobular organisation of the liver is further depicted in Figure 1.
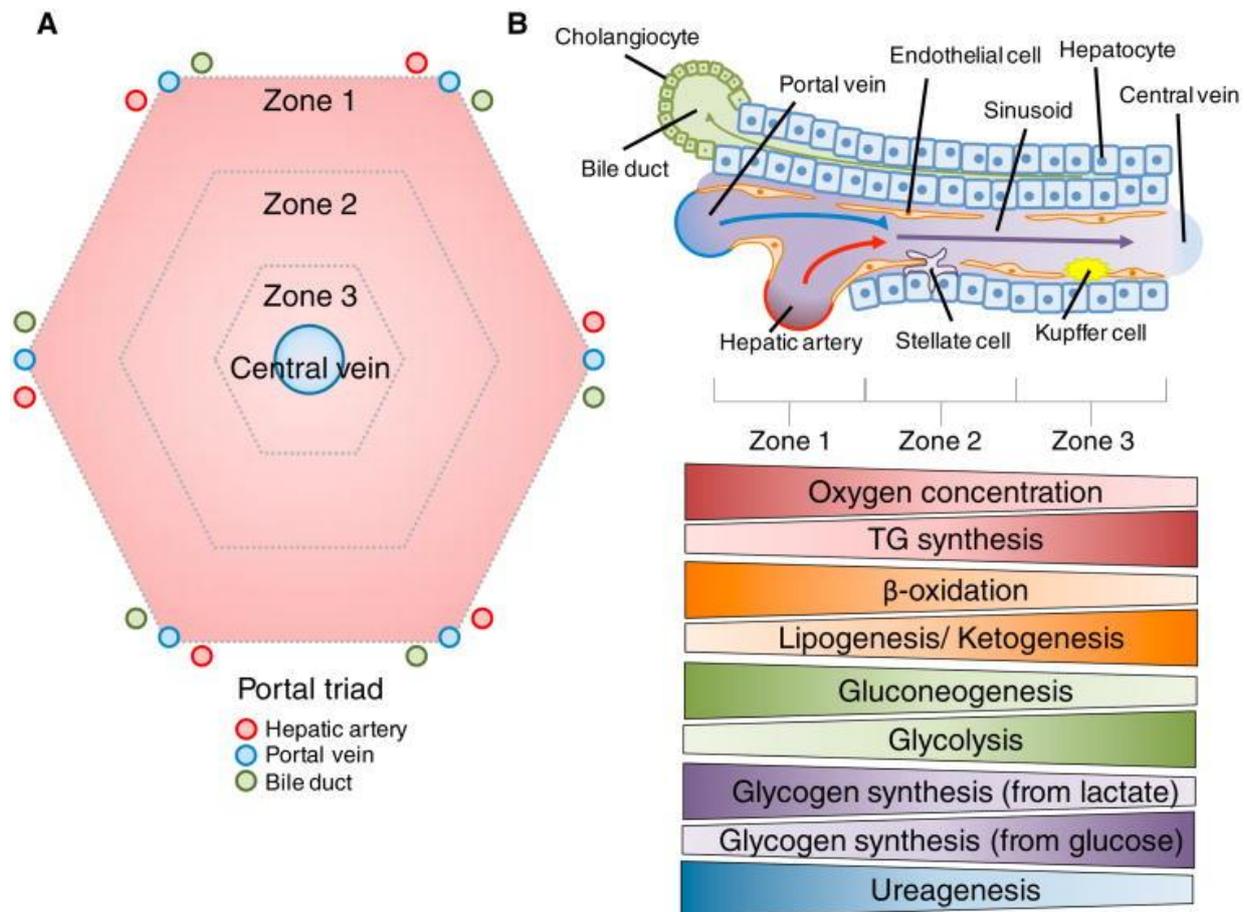
Figure 1. Diagram representing the hexagonally shaped Hepatic lobule (A). Each hepatic lobule has triads of portal vein, bile duct, and hepatic artery branches running along them. Nutrient-rich blood drained from the intestines through the portal hepatic system mixes with oxygenated blood from the hepatic artery and through the sinusoidal network of the lobule, draining into the central vein. Due to many different metabolites and compounds, such as different hormones, nutrients, oxygen, and materials, at varying concentrations numerous gradients are created. Illustration of liver cell organisation and gradient zonation (B). The sinusoid contains a variety of cell types, such as stellate cells, endothelial cells, Kupffer cells, hepatocytes, and biliary epithelial cells (cholangiocytes). Most liver metabolic processes are carried out by hepatocytes. Instead of forming tight connections, the endothelial cells of the liver produce networks of sieve plates. This produces a thin layer of protection between the hepatocytes and the blood in circulation. The aforementioned gradients are not static processes

but show dynamic changes influenced by periods of fasting, fed state and pathological changes. Source: Trefts E, Gannon M, Wasserman DH. The liver. Curr Biol. 2017;27:R1147-R1151.

1.1.2.3. Blood Supply

The hepatic blood supply originates from the celiac trunk which merges into the gastroduodenal tract and towards the *porta hepatis* as the proper hepatic artery. In the liver, the proper hepatic artery divides into left and right hepatic arteries(3). Meanwhile, the venous blood supply passes from the gastrointestinal tract into the liver via the portal vein(4). Via sinusoids, mixed artery and venous blood travel from portal areas to the central vein. Columns of hepatocytes that stretch from the portal region to the central vein make up the hepatic cords or plates (4).

1.1.2.4. Hepatocyte

Structurally, the liver comprises parenchymal cells - hepatocytes and non-parenchymal cells, including Kupffer cells, endothelial cells, HCS, pit, and biliary endothelial cells (5).

Making up more than half of the liver mass are hepatocytes, while biliary epithelial cells and stellate cells are the rest. Embryologically, hepatocytes and biliary epithelial cells are derived from the endoderm, whereas stromal, stellate, Kupffer cells, and blood vessels originate from the mesoderm. Fate mapping studies in mice have shown that the embryonic liver starts developing at embryonic day 8.0 and originates from the ventral foregut endoderm. The cells of early liver development are called hepatoblasts and are still bipotential, meaning they will develop into different cell types. Their location determines this development. Hepatoblasts next to the portal veins will differentiate into biliary epithelial cells, which will make up the intrahepatic bile duct lining. Hepatocytes located in the parenchyma differentiate into functional hepatocytes. From embryonic day 13, the maturation of the hepatocytes and extrahepatic cells starts growing into a functional and structural network of hepatic and extrahepatic structures, which will develop into the Liver tissue architecture of the mature liver.

As mentioned above, the endoderm not only gives rise to hepatocytes alone but also to biliary, gastrointestinal, and respiratory epithelial lining, glandular cells of the lung, thyroid, thymus, and pancreas. The endoderm and mesoderm differentiation is initiated through the transforming growth factor beta (TGFB) growth factor Nodal. Lower doses of Nodal induce mesodermic differentiation, and high doses of Nodal induce endodermic differentiation. This

signaling pathway stimulates the endoderm transcription factors *Sox17* and *Foxal1-3*. The differentiation between foregut and hindgut in the endoderm development is controlled by secretion and repression of fibroblast growth factor (FGF), wingless-related integration site (Wnt), bone morphogenetic proteins BMP, and retinoic acid (RA). These proteins create an interplay between their area of secretion. FGF4 and *Wnt* promote hindgut development when expressed from the posterior mesoderm, but their secretion needs to be inhibited in the anterior endoderm to promote foregut development. *Sfrp5* is responsible for the *Wnt*-inhibition in the foregut regions, which is vital as only the foregut can turn into the liver. Additionally, *Wnt2bb* from the lateral plate mesoderm is required for hepatic development in zebrafish, and *Wnt2* and *Wnt2b*, also from the lateral plate mesoderm, are expressed in mice during induction of hepatic development with an unknown role as of now.

The liver bud changes morphologically from embryonic day 8.5-9.0 and starts to express liver-specific genes (*albumin, alpha fetoprotein (AFP), and hepatocyte nuclear factor 4 alpha (HNF4A)*) from its epithelium. Between embryonic day 9.5 and embryonic day 15, the liver bud continues to undergo significant growth and increase in size and turns into the main organ for hematopoiesis in the fetus. This vital role of hematopoiesis is shown to be affected in many known gene mutations via inhibiting hepatoblast development and/or promoting apoptosis, which often leads to severe anemia and high lethality for embryos. The *septum transversum* mesenchyme and hepatic mesenchyme control the signaling for hepatoblast migration, proliferation and survival. Both secrete a variety of growth factors, such as FGF, BMP, Hepatocyte growth factor HGF, Wnt, TGFB, and RA. Although previously mentioned that Wnt/β-Catenin inhibits liver development in the early endoderm foregut and hindgut differentiations by embryonic day 10, β-catenin shows the opposite action and promotes liver growth in the liver bud. Indirectly, FGF and HGF signaling also stimulate the Wnt/β-catenin activity by stimulating the same intracellular kinase signaling chain of Mitogen-activated protein kinase (MAPK), c-Jun N-terminal kinase (JNK), and Phosphoinositide 3-kinases (Pi3K) (6).

1.1.3. Physiology of Liver

The liver is an essential organ with multiple endocrine, exocrine, and metabolic functions. Some of its vital functions are bile production, dietary compound metabolism, detoxification, the storage of glycogen and blood glucose regulation, and the production and release of serum proteins and clotting factors (6).

The ability of the liver to store, synthesise, metabolise, and release glucose is maintained throughout all stages of life. The liver switches between net glucose output and input states depending on fasting and feeding. Feeding leads to reduced hepatic glucose output from glycogen stores and an increase in insulin, causing a glycogenic response that increases hepatic glycogen stores. The opposite happens in fasting states; levels of insulin drop and glucagon rise, which leads to gluconeogenesis and the breakdown of glycogen to release glucose into the bloodstream. Pathology in this process is associated with diseases such as metabolic syndrome, non-alcoholic fatty liver disease and cardiovascular disease, mainly through the mechanism of insulin resistance (2).

Lipid and lipoprotein uptake, synthesis, packing, and secretion are all carried out by the liver. To facilitate fatty acid absorption into the bloodstream through the lymphatic system. The liver can use fats as an internal energy source through oxidative pathways. It can also release ketogenic products to supply energy to other organs, which is especially helpful during periods of intense fasting or very low carbohydrate consumption. The liver is crucial for supplying the body with lipid substrates, such as the skeletal muscle for energy production or the adipose tissue for storage. Many lipid-soluble vitamins cannot be absorbed without normal liver function (2).

The liver oversees producing 85–90% of circulating proteins, albumin being the most prevalent, making up 55% of the total protein in plasma. Albumin is necessary for maintaining blood volume and acts as a carrier protein for most hormones, lipids and even electrolytes. Acute-phase proteins, growth factors, and other vital proteins are also secreted by the liver. Furthermore, the liver is highly capable of metabolising the amino acids that make up proteins and breaking them down. The liver efficiently uses and excretes proteins using the urea cycle, which leads to the excretion of toxic urea buildup. Amino acids can also be used as an alternative in gluconeogenesis for glucose homeostasis by donating their carbon skeleton as substrates, useful in extreme states of fasting (2).

One remarkable function of the liver is its regenerative potential; up to 70% of liver tissue can be completely removed and regenerated by healthy liver tissue. Unfortunately, in diseases where hepatocytes are severely or permanently damaged, such as liver cirrhosis or hepatitis, this regenerative function is partially impaired or completely inhibited. The regeneration of the liver is mainly mediated by mature hepatocyte proliferation, although in the aforementioned disease states, the proliferation is inhibited, and hepatic progenitor cells are

activated. These progenitor cells are bipotential oval cells turning into hepatocytes or biliary epithelial cells induced by the same *Wnt*, *HGF*, and *FGF* pathways as during liver embryonic development (6).

1.2. Comparative anatomy of the Liver between mouse and human

The liver of a mouse is proportionally larger than that of a human, weighing approximately 1500 grams and making up 2% of body weight. A mouse liver normally weighs 2-3 grams and represents 3-5% of total weight. The liver in mice occupies a higher fraction of the subdiaphragmatic region than in humans, with the liver in humans being limited to the right superior abdominal quadrant. There are four lobes in the mouse liver: the right, left, middle, and caudate.

The gallbladder protrudes beneath the small central isthmus that connects the two symmetrical pyriform wings that make up the mouse median lobe. The human liver, on the other hand, consists of four partially divided lobes: the right, left, caudate, and quadrate. The human liver is a complex structure, with the portal vein, hepatic artery, and hepatic duct entering and leaving through the porta hepatis. Furthermore, the human liver is surrounded by a collagenous capsule called Glisson's capsule, which has notable peritoneal ligaments, including the coronary ligament, which connects the liver to the diaphragm, and the falciform ligament, which separates the right and left lobes. Such fine-grained connective structures are not described in mice, and the liver's anatomical structure seems simpler than the intricate lobular and ligamentous arrangement in humans.

Moreover, mice lack the abdominal ligaments that clearly define the lobes in the human liver. In humans, the liver is supported by the hepatic veins that link to the inferior vena cava, ensuring its location in the upper abdominal cavity. In contrast, the mouse liver's left lobe is the largest and is frequently the site of histological samples. This variation in anatomical form and location emphasizes the functional and physiological distinctions between the livers of mice and humans (2).

1.3. Comparative histology of the Liver between mouse and human

Both in humans and mice, the liver's complex structure is a reflection of its essential function in detoxification and metabolic control. The main working cells of the liver, called hepatocytes, are arranged into plates held up by an intricate web of reticulin and other stromal

components. The liver lobules' structural foundation comprises these plates, which extend outward from the central artery. This configuration ensures that hepatocytes and the blood supply are in proximity, which maximises the liver's metabolic efficiency. The liver's various activities depend on the opposite direction that blood and bile flow through it. Nutrients, oxygen, and metabolic waste product-carrying mixed arterial and venous blood flow through complex sinusoids from the portal areas to the central vein. Hepatocytes produce bile to help with digestion and waste removal; this bile is directed towards portal regions via canaliculi lined with specialised microvilli. Both species share the same hepatic lobular architecture, defined by hepatic cords or plates scattered with sinusoids. These cords are structurally supported by reticulin, which maintains the integrity of the liver's functional units. Furthermore, the bile's counter-current flow in relation to blood optimises the liver lobule's metabolic processes(4).

Although the overall liver anatomy is the same, humans and mice have several significant differences. The presence of a more significant collagenous network supporting the portal regions in humans suggests that the mechanical characteristics and tissue organisation of humans may differ from those of mice. Human hepatic plates are primarily single-cell in nature, which allows for fine metabolic regulation and functional organisation. On the other hand, mice might show postprandially compressed hepatocytes, which would lead to a less clear cellular cord demarcation, particularly in particular lobular areas. The tiny tubular channels known as bile canaliculi, which connect hepatocytes, are essential to the secretion and movement of bile. These structures ensure the effective removal of waste items from the liver by receiving bile from hepatocytes and finally converging into bile ducts. The lobule's outer canals, known as hepatic stem cells, are home to fuzzy progenitor cells. These cells can multiply in reaction to damage and have the ability to regenerate, which adds to the liver's amazing ability to heal and regenerate itself (4).

1.4. *Yotari* mice

The *yotari* (*yot)* and *reeler* mice are phenotypically very similar, showing unstable gait and tremor, short life span, and hypoplastic cerebella with histological structure abnormalities. Due to the phenotypical similarity, it was believed that the novel *yot* mice were also *reeler* genotypes, lacking the *reelin* gene. Besides the similarity of *yot* and *reeler* mice in later post-natal life, in the first few weeks, *yot* mice cannot be easily distinguished from non-mutant litter mates. Only after a few weeks do they exhibit significantly reduced growth and size, and

additionally, their unstable gait tends to fall over frequently. Experiments showed that *yot* mice crossed with *reeler* mice produced normal offspring, which did not support the theory of the same mutation being present. Further investigations proved that *yot* mice express mRNA for *reelin* and produce the reelin protein (using northern blotting and immunohistochemistry with CR-50 monoclonal antibodies(7).

Multiple other genes that are known to cause laminar structural abnormalities in the brain were also tested in the *yot* mice, *cyclin-dependant kinase 5*, p35, LISI, *platelet-activating factor acetylhydrolase 1b* all were shown to be normal in *yot* mice using western blotting and antibodies directed at the proteins as mentioned above. At the time of emergence, it was not known yet which gene mutation affected the *yot* mice, but it was thought to be on the same signaling pathway or in some way connected with reelin. When *yot* mice first appeared, they were the offspring of a male chimeric mouse that was supposed to create an inositol 1,4,5-trisphosphate receptors (*IP3R1) knockout* mouse. Its offspring were proven to express the *IP3R1* gene and are distinguishable from other *IP3R1 knockout* mice through this gene. Therefore, *yot* mice have genetic mutations independent of *IP3R1* (7).

Today, it is known that *yot* mice have a mutation in the *disabled 1* (*Dab1*) gene, which causes the production of a dysfunctional Dab1 protein. The exact mutation was demonstrated by Kojima et al. to be caused by a replacement of gene sequence by a long interspersed nuclear element. This substitution eliminates three introns and two exons by substitution. The long interspersed nuclear element that is substituted consists of 962 nucleotides and is truncated at 5' and 3' ends. This new knowledge of the precise gene mutations enables us to identify and differentiate between *yot*, wild-type and heterozygous mice. The autosomal recessive mutation of *Dab1* causes homozygous *Dab1 yot* mutant mice, also known as *Dab1yot* (*yot/yot*) mice, to exhibit *reeler*-like phenotypes, including cerebral cortex, hippocampus, and cerebellar histological abnormalities. The hippocampus of *yot/yot* mice develops abnormally, with granule cells and pyramidal cells scattered diffusely in hazy multiple layers instead of forming orderly rows. The reason behind the axons of granule cells in *yot/yot* animals not actively extending to connect with neighbouring regions could be attributed to the placement failure of both pyramidal and granule cells, as well as poor synaptogenesis. We discovered that the yot/yot mice's pyramidal cells and hippocampus granule cells both expressed proteins that reacted with the anti-Dab1 antibody (12). For the mammalian brain to correctly form, the migration of neurons needs to be precisely choreographed. Laminar structures need to be

formed in the forebrain cortices and cerebellum. The formation of these structures is severely disrupted in reelin mutations due to faulty neuronal migration, leading to ataxia. Phenotypically similar mice have been created since the discovery of the *reelin* mutation. These novel mice, *yot* and *scrambler*, also suffer from ataxia and early death. Unlike *reeler* mice, it is proven to be a mutation in the drosophila gene disabled that is responsible for the *yot* phenotype. This mutation causes the expression of mutated *mdab1* messenger RNA and a reduction or complete loss of mDab1 protein expression. The *mDab1* phosphoprotein acts as an intracellular adaptor in protein kinase pathways. It has also been proven that mdab1 is expressed in the same cells that express reelin; in addition, the similarity in phenotype indicates that *mdab1* and *reelin* both have a function in signalling and regulating cell migration in brain development (9).

1.5. Wnt signaling pathway

The Wnt pathways are a network of interrelated signalling systems that are essential for regulating the destiny of cells during embryo development. Although the fruit fly *Drosophila* is where these pathways were initially discovered, a variety of developmental processes in both vertebrate and invertebrate embryos benefit from their significance. Cell patterning and differentiation required for developing many structures, including limbs, the nervous system, the skeleton, the lungs, hair, teeth, and gonads, are established by Wnt signaling (10). The Wnt pathway is further illustrated in Figure 2.
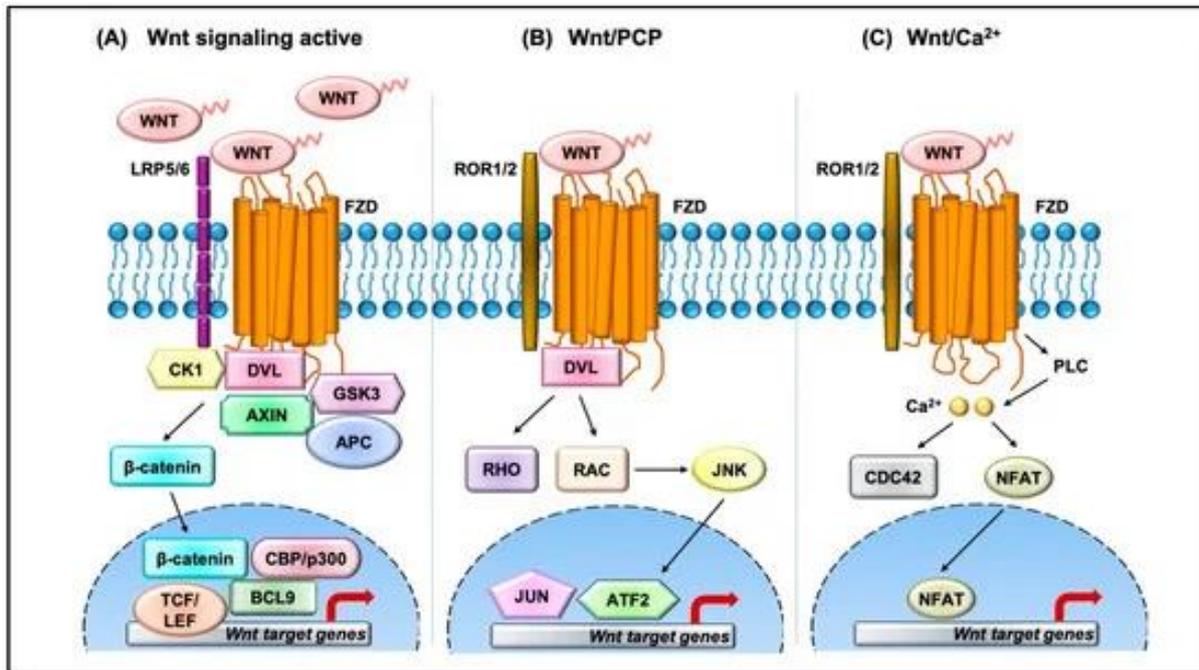
Figure 2. Wnt ligands (Wnt3A and Wnt1) are secreted and bind to LRP co-receptors and Frizzled (FZD) receptors in the canonical Wnt pathway (A). Subsequently, these receptors are phosphorylated by Casein kinase 1 (CK1) and Glycogen Synthase Kinase 3 Beta (GSK3B), which attracts Dishevelled (DVL) to the plasma membrane and starts the activation process. The DVL signalosome causes the β-catenin destruction complex (Axin and Adenomatous polyposis coli (APC)) to be sequestered and inhibited, which raises the quantities of stabilised β-catenin in the cytoplasm. β-Catenin translocates into the nucleus, where it joins with T-cell factor (TCF), lymphoid enhancer factor (LEF), and other histone-modifying coactivators like CREB-binding protein (CBP)/p300 and B-cell CLL/lymphoma protein 9 (BCL9) to form an active complex. This complex activates the transcription of Wnt target genes, increasing cellular processes like cell proliferation, differentiation and renewal of stem cells. The Wnt/PCP pathway involves the recruitment of DVL to the plasma membrane by Wnt ligands binding to FZD and co-receptors (B). DVL further activates JNK, triggering cytoskeletal rearrangements. The non-canonical Wnt/Ca2+ pathway is initiated by G-protein-triggered phospholipase C (PLC) activity and the Wnt-FZD-ROR complex, which causes an intracellular Ca2+ influx (C). A variety of transcriptional reactions further activate CDC42 and cause calcium-dependent cell motility and polarity (red arrow). Source: Sharma M, Pruitt K. Wnt

pathway: An integral hub for developmental and oncogenic signaling networks. Int J Mol Sci. 2020:21:1-24.

1.6. Canonical Wnt Signaling

The family of secreted growth factors known as Wnt proteins binds to receptors belonging to the FZD and Lipoprotein receptor-related protein (LRP) families, which are connected to the Smoothened protein (SMO). DVL is a cytoplasmic protein that gets activated when Wnt proteins attach to these receptors. APC, the protein kinase GSK-3β, axin, and other proteins are all involved in this activation-induced protein complex inhibition. GSK-3β phosphorylates β-catenin under normal circumstances, designating it for ubiquitination and destruction. Wnt signalling, on the other hand, stops this phosphorylation, which raises the amount of β-catenin in the cell(10).

The Smoothened protein is linked to the Frizzled and LRP families of receptors, which are bindable by the Wnt protein family of secreted growth factors. Cytoplasmic protein DVL is activated upon attachment of Wnt proteins to these receptors. This activation-induced inhibition of protein complexes involves APC, the protein kinase GSK-3β, axin, and other proteins. Under normal circumstances, GSK-3β phosphorylates β-catenin, marking it for ubiquitination and elimination. Conversely, Wnt signalling prevents this phosphorylation, increasing the cell's β-catenin levels (10).

1.7. Non-canonical Wnt signaling

Noncanonical Wnt signalling involves Wnt5a type ligands, including Wnt4, Wnt5a, Wnt5b, Wnt6, Wnt7a, and Wnt11. It is β-catenin-independent. Different from the canonical pathway, this one mainly affects cellular migration and polarisation. The Wnt/calcium (Ca^{2+}) route and the Wnt/planar cell polarity (PCP) pathway are two of its sub-pathways (12).

Like the canonical system, the Wnt/PCP pathway involves several coreceptors, including Protein Tyrosine kinase 7 (PTK7), Muscle-specific kinase (MUSK), ROR1/ROR2, related to receptor tyrosine kinase (RYK), syndecan, and glypican, in addition to Fz receptors to bind Wnt ligands. It also involves VANGL planar cell polarity protein 2 (Vangl2) and Cadherin EGF LAG seven-pass G-type receptor 1 (Celsr1) receptors, though it's unclear exactly how these ligand-receptor interactions work. In the Wnt/PCP pathway, Fz receptors phosphorylate Dvl upon ligand binding, which in turn attracts Invs (12).

1.8. Polarization and proliferation of epithelium

Additionally, the non-canonical Wnt pathway dictates cell polarisation. Following an interaction between the polarity protein Par6 and Dvl, phosphorylated Dvl attracts Smurf, which binds to Par6. Prickle, an inhibitor of Wnt/PCP signalling, is marked for proteasomal destruction by Smurf by ubiquitination. Dvl can attach to the Dvl-associated activator of morphogenesis (DAAM) by this degradation, activating RhoA but not Rac1 or Cdc24. Profilin is also activated by DAAM. JNK is activated by Rac1, and this phosphorylates and activates c-Jun to start the production of genes, as well as phosphorylating CapZ-interacting protein (CapZIP). Rho associated protein kinase (ROCK) and Diaphanous-related formin-1 (DIA1) are activated by Ras homolog family member A (RhoA), and ROCK then triggers the myosin II regulatory light chain (MRLC). Actin polymerization is facilitated by CapZIP, Myosin regulatory light chain (MRLC), DIA1, and profilin and is necessary for cell polarity and migration (12).

1.9. Disabled 1

Disabled 1 (Dab1), an intracellular adaptor protein crucial for Reelin signal transduction, plays a fundamental role in orchestrating neural network formation and neuronal positioning during brain development in mice. Upon Reelin binding, Dab1 undergoes tyrosine phosphorylation, primarily facilitated by the Src-family kinases Proto-oncogene tyrosine-protein kinase Fyn (Fyn) and Proto-oncogene tyrosine-protein kinase Src (Src), subsequent to its interaction with lipoprotein receptors such as apolipoprotein E receptor 2 (ApoER2) and very-low-density-lipoprotein receptor (VLDLR)(13,14). This phosphorylation event initiates various signaling cascades, including the recruitment of proteins containing Src Homology 2 domain (SH2) domains, crucial for pathways like Wnt signaling. Additionally, Dab1 phosphorylation is vital for neuronal migration, particularly somal translocation, a process that involves the activation of the Crk/C3G/Rap1 pathway, ultimately facilitating neuronal interaction with Reelin-producing Cajal cells through adhesion molecules like Nectins and N-Cadherin. Furthermore, Dab1 signaling influences the orientation of migrating neurons transitioning from multipolar to bipolar morphology, crucial for their radial migration into the cortical plate (13). Beyond its role in neuronal positioning, Dab1 is implicated in diverse cellular functions. It interacts with receptors such as ApoER2 and VLDLR, not only in neuronal cells but also in endothelial cells during brain vascularization, where it becomes phosphorylated upon Vascular endothelial growth factor (VEGF) binding to VEGF receptor 2

(VEGFR2). Moreover, Dab1 expression in the small intestine's crypt-villus axis suggests involvement in epithelial cell turnover, potentially regulating cellular homeostasis. Furthermore, Dab1's involvement extends to tumorigenesis, where it participates in a Reelin-independent pathway through interaction with epidermal growth factor receptors (EGFR), triggered by epidermal growth factor (EGF) phosphorylation. This interplay between Reelin signalling and other pathways, such as Notch, underscores the multifaceted roles of Dab1 beyond neuronal development, including implications in tumour growth and metastatic progression, particularly in colorectal cancer invasion and metastasis (13–15).

1.10. Inversin

Inversin (Invs) plays a crucial role both in canonical and non-canonical Wnt signaling (14). Invs is a cellular signaling protein involved in multiple pathways and roles. It is a member of a large family of ankyrin repeat-containing proteins. More than 12 are known. The human isoform contains 16 tandem ankyrin repeats and additionally two of each D-Box destruction domains and calmodulin-binding IQ domains. These D-Box domains play an integral role in Invs binding its target APC complex and in the degradation of Dishevelled. Its name comes from inversion, which is a key role of the protein in determining the left-right positioning of the body and organs. In animals lacking Invs *situs inversus* and other organ anomalies have been reported. The expression is known to be highest in the kidney and liver of adult specimens. It is known that Invs acts through the Wnt canonical pathway, acting as a molecular switch in different downstream pathways. It inhibits the canonical Wnt pathway via the degradation of cytoplasmic DVL protein and recruits DVL to the plasma membrane to polarise cells and promote cilia development (16–19). Sharma et al. found with quantitative trait localization, through pcy, cpk, jck, and bpk mouse models of human polycystic kindey disease (PKD), that *invs* is one of several genes inside a locus that contains one or more modifying genes. These results imply that, like β-catenin's biological role, isoforms of Invs may be involved in gene transcription and intercellular junction biosynthesis (20).

1.11. Dishevelled-1

The *DVL* gene was originally discovered in *Drosophila* mutants with asymmetrical hair and polarity in their bristles. In *Drosophila* and vertebrates, respectively, the *Dsh* gene (*Dsh/Dvl*) is crucial for segment polarity in the early stages of embryonic development. Following this, it was discovered that the vertebrate equivalent of the *DVL* genes was present

in humans (*DVL-1, DVL2, DVL3*) as well as mice (*Dvl-1, Dvl2, Dvl3*). DVL is a key player in the Wnt signalling pathway and regulates a number of biological functions, including as stem cell renewal, migration, differentiation, proliferation, survival, and polarity. This information spreading could start a signalling cascade that ends in either an impact that is β-catenin-independent or stabilises β-catenin (21).

Three conserved domains are present in all DVL proteins, from *Drosophila* to humans: the carboxyl-terminal Dishevelled, Egl-10 and Pleckstrin domain (DEP) domain, the central postsynaptic density protein (PSD95), Drosophila disc large tumor suppressor (DlgA), and zonula occludens-1 protein (PDZ), and the amino-terminal DIX domain. DVL contains two areas with positively charged amino acid residues in addition to these three domains. The first is a "basic region" that sits between the PDZ and DIX domains and comprises conserved serine and threonine residues. The second is located downstream of the PDZ domain and is known as a "proline-rich region." These conserved domains aid DVL channel signals into the canonical or non-canonical Wnt pathway and mediate protein-protein interactions (21).

DVL is a family of signaling proteins in the Wnt/B Catenin pathways. The three isoforms DVL 1, 2 and 3 are all cytoplasmatic proteins responsible for the phosphorylation of downstream proteins. DVL-1 is the major signaling protein in the Wnt Pathway. The signaling protein acts through DVL, binding its c-terminal Val-Trp-Val motif to membrane receptors crucial in its pathway. A lack of this functional DVL-Wnt pathway is known to cause early perinatal death due to kidney malformation. In addition, the DVL expression is linked to the growth of multiple malignant tumors (22–24).
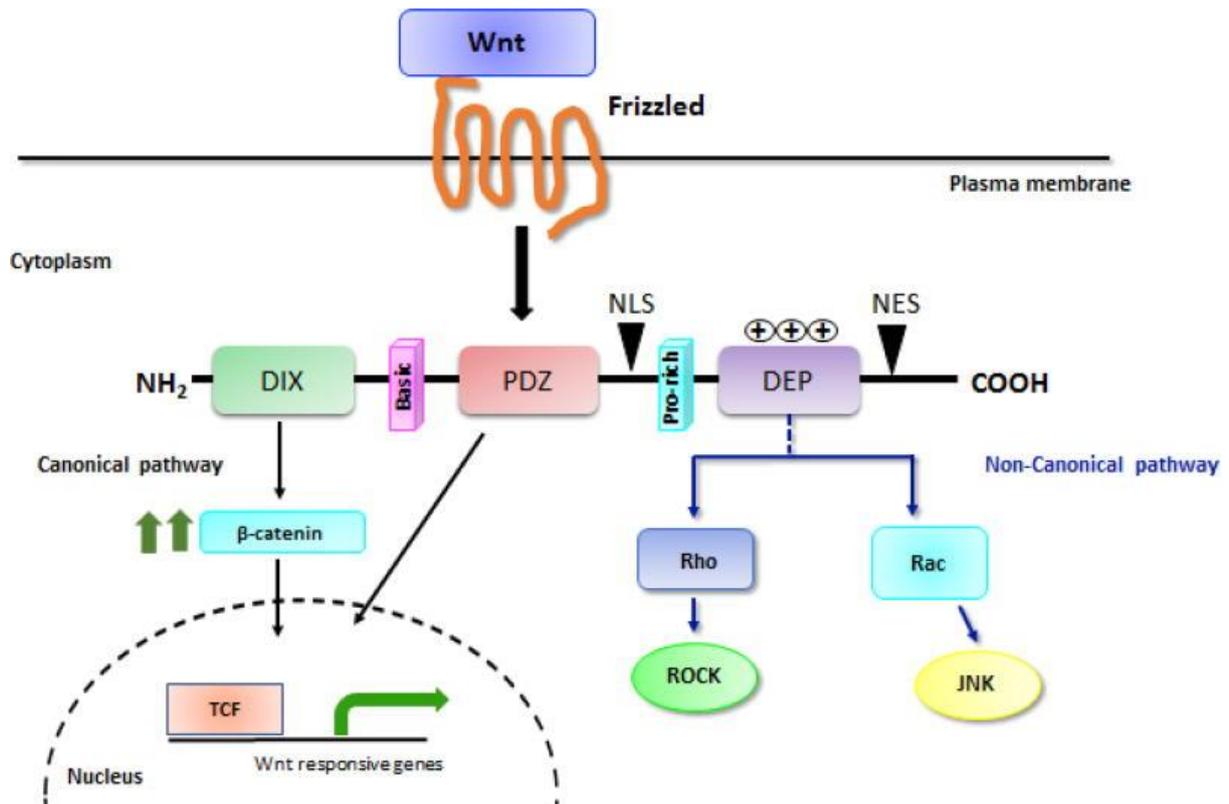
Figure 3. Three conserved motifs make up DVL: the carboxyl-terminal DEP domain, the central PDZ, and the amino-terminal DIX domain. Additionally, two areas containing positively charged amino acid residues, a nuclear export signal (NES) and a nuclear import signal (NLS), are present in DVL. While the DEP domain primarily controls the membrane location of DVL and spreads the non-canonical pathway (shown in blue arrows), the DIX and PDZ domains relay signals to the canonical pathway (shown in black arrows). Source: Sharma M, Castro-Piedras I, Simmons GE, Pruitt K. Dishevelled: A masterful conductor of complex Wnt signals. Cellular Signalling. Elsevier Inc.; 2018:47:52–64.

2. OBJECTIVES

This study aims to identify, using immunohistochemistry, if there are differences in the expression of Invs and DVL-1 protei in *yot* mice liver tissue compared to control mice. Possibly useful as foundational results used for further investigating molecular processes that underlie the emergence of hepatic dysfunction in the context of *Dab1* disruption, elucidating possible ramifications for hepatic physiology and associated treatment approaches.

3. MATERIALS AND METHODS

3.1. Ethics

The use of animals in this study was approved by the Guidelines for the Care and Use of Laboratory Animals at Shiga University of Medical Science. The study was approved by the University of Split School of Medicine's Ethical Committee and was carried out in accordance with the guidelines outlined in the Declaration of Helsinki (class: 003-08/16-03/0001, approval number: 2181-198-03-04-16-0024).

3.2. Sample Collection

Homozygous $Dab1^{-/-}$ yot mutant mice, who have an autosomal recessive mutation of the *Dab1* gene and exhibit tremors, an unsteady walk, and early death around the time of weaning, were employed in this experiment (25). The C57BL/6N wild-type mice and *yot* mice were housed in groups in standard polycarbonate cages with free access to food and water in a temperature-controlled environment ($23 \pm 2°C$). There were 12 hours of artificial light and 12 hours of darkness during the photoperiod. The PCR primers GCCCTTCAGCATCACCATGCT and CAGTGAGTACATATTGTGTGAGTTCC for *yot* and GCCCTTCAGCATCACCATGCT and CCTTGTTTCTTTGCTTTAAGGCTGT for wild type were utilised for genotyping. The gravid mice were sacrificed on embryonic days 13.5 (E13.5) and 15.5 (E15.5) in order to obtain their embryos. Three mice of each genotype (*yot* and wt) were studied at the time point in question. The animals were transcardially perfused with phosphate buffer saline (PBS, pH 7.2) and 4% paraformaldehyde (PFA) in 0.1 M PBS after being anesthetized with 1.5% sodium pentobarbital (26).

3.3. Immunofluorescence Staining

Using graded ethanol solutions (Sigma Aldrich, St. Louis, MO, USA), the tissue was first fixed and dried. It was then serially sliced into five-micron-thick sections, embedded in paraffin blocks, and mounted on slides. The appropriate preservation of tissue was confirmed by the hematoxylin-eosin (HE) staining of every tenth segment. After deparaffinization in xylol and rehydration in graded ethanol and distilled water, the mounted tissue samples were heated in a sodium citrate buffer (Sigma Aldrich, St. Louis, MO, USA) for 20 minutes at 95 °C in a water steamer. They were then gradually cooled down to room temperature. To avoid non-specific staining, a protein-blocking buffer (ab64226, Abcam, Cambridge, UK) was administered for 20 minutes after washing in 0.1 M PBS. The sections were incubated with primary antibodies overnight in a humidity chamber (Table 1). They were washed with PBS

the next day and then incubated with the appropriate secondary antibodies for an hour (Table 1). After giving the samples a thorough rinse in PBS, the nuclei were cover-slipped and stained with 4′,6-diamidino-2-phenylindole (DAPI) (Immuno-Mount, Thermo Shandon, Pittsburgh, PA, USA). Every primary antibody was diluted to the precise concentration in a blocking solution once the pre-adsorption test was finished. Sections were treated with the mixture following the addition of a sufficient amount of peptide antigen. Eliminating primary antibodies from the technique did not result in non-specific secondary antibody binding or false-positive results.

Table 1. Antibodies used for immunofluorescence

Antibodies		Catalog Number	Host	Dilution	Source
Primary	Anti-inversin	ab6187	Rabbit	1:100	Abcam (Cambridge, UK)
	Anti-dishevelled-1	Sc-8025	Mouse	1:50	Santa Cruz Biotechnology (Dallas,TX, USA)
Secondary	Anti-Rabbit IgG, Alexa Fluor r 488	711-545-152	Donkey	1:300	Jackson Immuno Research Laboratories, Inc., (Baltimore, PA, USA)
	Anti-Mouse IgG Rhodamine Red TM-X	715-295-151	Donkey	1:300	Jackson Immuno Research Laboratories, Inc., (Baltimore, PA, USA)

3.4. Data Acquisition and Analysis

An immunofluorescent microscope (BX51, Olympus, Tokyo, Japan) equipped with a Nikon DS-Ri2 camera (Nikon Corporation, Tokyo, Japan) was used to analyze the sections. Non-overlapping visual fields were recorded at a magnification of x40 and constant exposure

periods to determine the immunoexpression of proteins of interest. At least ten images of the embryonic liver structures were taken at E13.5 and E15.5. All analyzed images were processed with ImageJ software (NIH, Bethesda, MD, USA) and Adobe Photoshop (Adobe, San Jose, CA, USA) [37].

Quantitative estimation of immunoreactivity was obtained using subtraction of the median filter and color thresholding to calculate the section percentage area covered by the positive signal.

Any level of nuclear, cytoplasmic, or membrane staining was considered positive. Negative cells were categorized as cells with the absence of any immunoreactivity.

3.5. Statistical Analyses

The statistical analysis was performed using GraphPad Prism 9.0.0 software (GraphPad Software, San Diego, CA, USA). To identify significant differences in the area percentage of positive cells, immunoexpression was compared by a two-way ANOVA test and Tukey's multiple comparison test between epithelium and mesenchyme at E13.5 and E15.5 of control specimens and *yot* mice. Mean value standard deviation (SD) was used to represent the percentage of positive cells, with $p < 0.05$ being the threshold for statistical significance.

4. RESULTS

This research utilized *yot* $(Dab1^{-/-})$ and wild-type (control) mice liver samples to investigate the protein expression patterns of Invs and Dvl-1 at gestation days E13.5 and E15.5. The study concentrated on the co-expression of Invs and Dvl-1. The findings indicated positive expression patterns, albeit with intensity, distribution, and quantity differences.

4.1. Hematoxylin-eosin (H&E) staining of the embryonic *yotari* and wild-type mice liver

By E13.5, the liver has attained its definitive embryonic structure, but it will continue to increase in size during the next stages of development. Following this stage, the observed alterations in the growing liver predominantly occur at the cellular level. This stage signifies the highest point of hematopoietic activity in the liver. Under high magnification, hematopoietic cells are the predominant feature in the field (Figure 4). Hepatoblasts have minimal intercellular communication and a larger density in the liver's outside regions than in the central region. Megakaryocytes are abundant throughout this developmental stage (Figure 4). Erythroblastic islands are present in various locations throughout the liver. An island's anatomic unit comprises a central macrophage positive for F4/80, surrounded by one or more concentric rings of mature erythroblasts.

The liver at E15.5 has a comparable structure to the E13.5 stage. Hepatic hematopoiesis begins to decline during this period. A significant number of the nucleated red blood cells that were previously present have now expelled their nuclei, resulting in a wide range of erythrocyte sizes. Megakaryocytes are still observed in abundance at this stage. Sections of the liver at E15.5 show the *ductus venosus*, caudal vena cava, and portal vein.

H&E staining showed no morphological differences between the livers of the control and *yot* specimens (**Figure 4**).
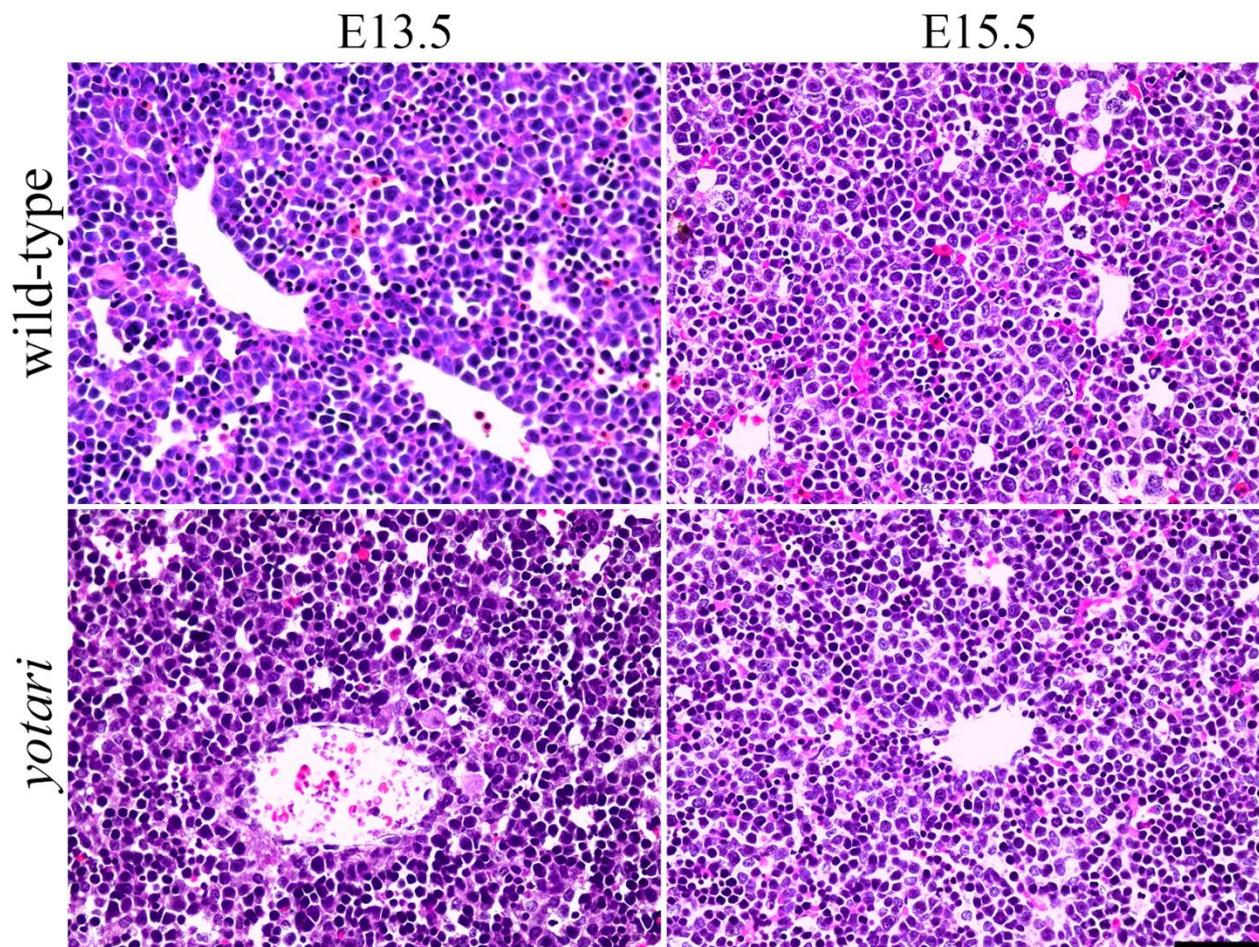
Figure 4. Hematoxylin-eosin (H&E) staining of the wild-type mice specimens and *yotari* liver at the embryonic day 13.5 (E13.5) and 15.5 (E15.5). Images were taken at a magnification of ×40. The scale bar is 40 μm.

4.2. Double immunofluorescence staining of the Inversin in embryonic *yotari* and wild-type mice liver

Invs was noticed as a green diffuse staining with widespread cytoplasmic distribution in the maturing hepatocytes (**Figure 5**). The percentage of Invs-positive cells showed a distinct pattern. In wild-type mice, the percentage of Invs-positive cells increased from gestation day E13.5 to E15.5, while in *yot* mice, it decreased during the same observed period. Comparing the differences in the area percentage of Invs-positive cells, we found a significantly higher Invs expression in the *yot* at E13.5, which decreased significantly at E15.5 compared to wild-type mice (**Figure 6**).

4.3. Double immunofluorescence staining of the Dishevelled-1 in embryonic *yotari* and wild-type mice liver

Dvl-1 is observed as a red diffuse cytoplasmic staining with the widespread cytoplasmic distribution in the maturing hepatocytes (**Figure 5**).

Dvl-1 showed negligible variation in the expression pattern between the two mice phenotypes at both observed time points. Generally, the percentage of cells positive for Dvl-1 was higher in the wild-type mice compared to the *yot* mice. Over the observed period from E13.5 to E15.5, the expression trend demonstrated a decrease in the percentage of Dvl-1 positive cells in the control mice and an increase in the *yot* mice (**Figure 6**).

The co-expression of the Inversin and Dishevelled-1 is noticed in the cytoplasm of the maturing hepatocytes (**Figure 5**).
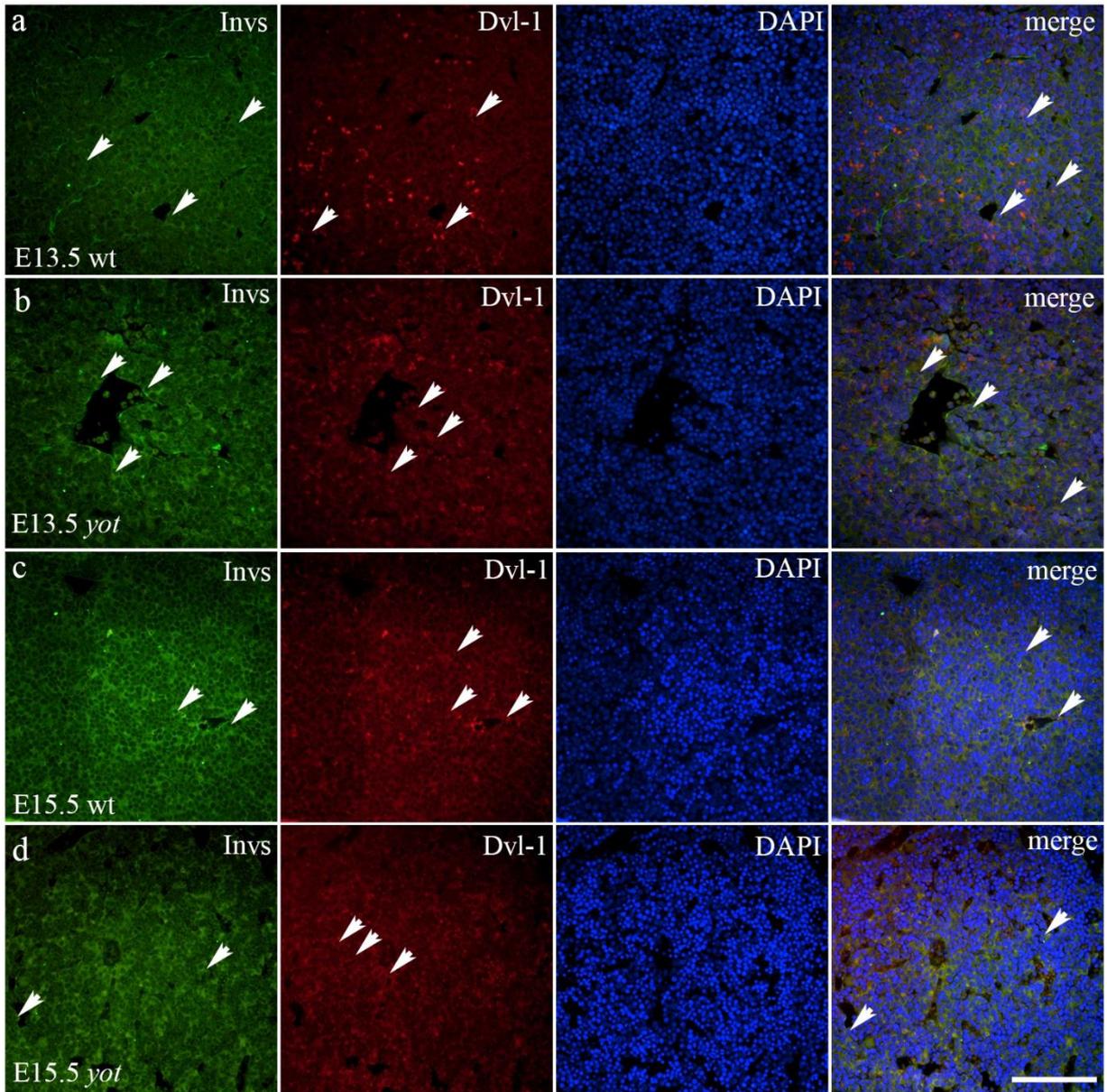
Figure 5. Immunofluorescence staining of Inversin (Invs), Dishevelled-1 (Dvl-1) merged with 4′,6-diamidino-2-phenylindole nuclear staining image (DAPI) in the developing wild-type specimens (wt) and *yot* mice liver (a–d). Invs and Dvl-1 comparison between liver at embryonic days 13.5 (E13.5) and 15.5 (E15.5) (a–d). Positive staining of Invs and Dvl-1 (arrows) is shown in the liver (a–d). Co-expression of merged images of all panels (arrows). Magnification ×40, scale bar 50 μm.
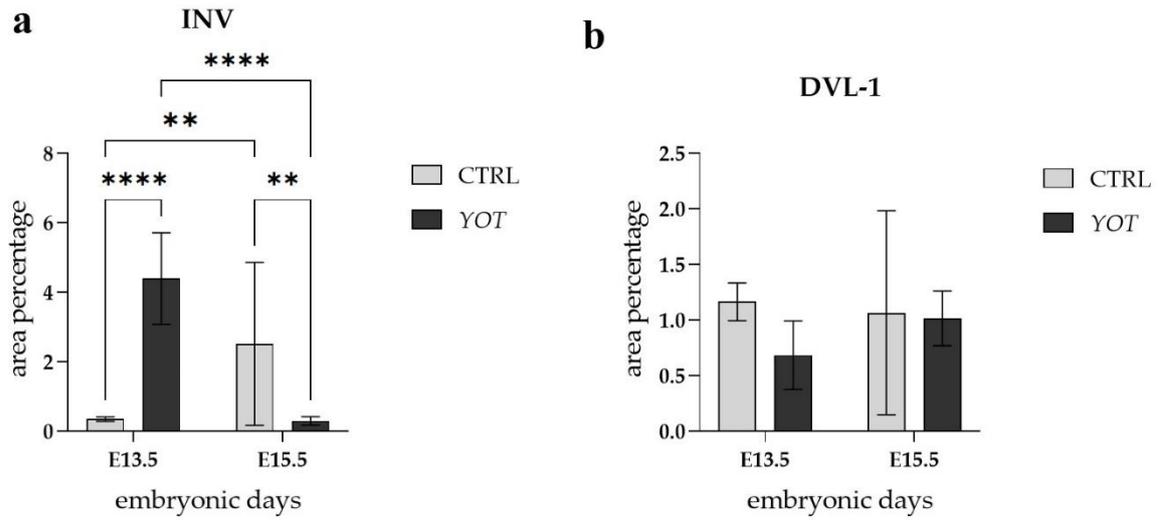
Figure 6. The area percentage of INVS and Dvl-1 in control specimens (ctrl) and *yot* mice at E13.5 and E15.5. of developing liver. Data were displayed as the mean ± SD (vertical line) and analyzed by a two-way ANOVA test followed by Tukey's multiple comparison test. Significant differences are indicated by ** $p < 0.01$; **** $p < 0.00001$.

5. DISCUSSION

This study examines the impact of genetic *Dab1* mutation affecting the Wnt signaling pathway on the development of an essential organ - the liver. Using *yot* (*Dab1$^{-/-}$*) mutant mice, the research focuses on the expression profile of Invs and Dvl-1 in liver development. As previously stated, the *Dab1* gene plays a crucial role in mice's brain and kidney development. It regulates several pathways, such as Reelin/DAB1 and Wnt, which affect cell fate and differentiation.

Although there is no existing research on Invs expression during liver development in *yot* mice, significant studies have been conducted on mice and zebrafish kidney development.

In zebrafish, the protein Invs regulates different Wnt signaling pathways. Specifically, it stops the canonical Wnt pathway by causing the degradation of cytoplasmic Dvl. At the same time, it is necessary for non-canonical Wnt signaling, which controls certain processes related to the development of *Xenopus laevis* embryos and animal cap explants (16). Invs expression is also crucial for the normal development of the kidneys in zebrafish. When Invs is lacking, the fish develop cysts in their kidneys. However, these cysts can be prevented by the presence of a similar protein called diversin, which acts as a switch molecule. This suggests that inhibiting canonical Wnt signaling is necessary for proper kidney development (27).

A recent study by Perutina et al. discovered that Invs expression generally increases during normal kidney development, with higher expression in *yot* mice as the kidney matures (14).

Similarly to animal models, it is well known that abnormalities in the Wnt signaling, caused by mutations in proteins like Invs and disrupted DVL-1 expression, can lead to kidney damage, including fibrosis and cystic kidney diseases in humans. Targeting Wnt/β-catenin signaling shows potential in treating kidney diseases. Furthermore, interactions between TGF-β, Wnt, and cilia can influence kidney health (14).

Our results demonstrate a distinctive expression pattern of Invs and Dvl-1 during embryonic liver development, suggesting potential implications for congenital anomalies and disease progression associated with dysregulated Wnt signaling. Detailed changes in protein expression levels during critical stages of liver development were observed in *yot* mutant mice and controls using immunofluorescence staining.

For wild-type mice, there was an increase in the percentage of Invs-positive cells from gestation day E13.5 to E15.5, whereas in *yot* mice, there was a decrease over the same timeframe. When comparing the variations in the area percentage of Invs-positive cells, we noted a notably higher expression of Invs in *yot* mice at E13.5, which significantly declined by E15.5 compared to wild-type mice. The observed increase in Invs expression at E13.5 suggests a potential role in early liver development in *yotari* mice. The subsequent decline by E15.5 may indicate regulatory mechanisms or developmental transitions specific to *yotari* mutants. The possible significance of Invs expression differences could be elucidated further by what we already know about the role of Invs, specifically its role in liver development and function.

Known anomalies highlight the significance of Invs in hepatobiliary development and liver function. The deletion of the *Invs* gene in the *Invs* animal model has shown impaired bile flow and *situs inversus* caused by aberrant gastrointestinal rotation during embryonic development, which is characterised by cholestasis and hyperbilirubinemia (28). The role of Invs is also known in the non-canonical Wnt Pathway by recruiting Dvl proteins for cytoskeletal changes responsible for cellular polarity(16). As mentioned below, the effect on the canonical Wnt pathway and its inhibition of β-catenin can be further elucidated and possibly correlated with already known roles in liver function and pathology. The protective function of β-catenin is known in hepatic pathology by controlling the inflammatory axis and reducing oxidative stress. In mice lacking β-catenin, severe liver disease such as steatohepatitis, fibrosis and hepatocellular is observed after iron overload (29). There is theoretical evidence of the therapeutic potential of cholestatic liver injury alleviation through modulation of the inflammatory response through inhibition of the Wnt signalling pathway. Increased expression of β-catenin and other target genes demonstrates how amplified Wnt signalling exacerbates liver inflammation and damage under cholestatic circumstances. Wnt pathway inhibition greatly reduces inflammation via the reduction of Nuclear factor kappa-light-chain-enhancer of activated B cells (NF-kB) pathway and levels of Tumor necrosis factor-alpha (TNF-a) and Interleukin 6 (IL-6). A reduction in liver inflammation markers, Bilirubin and Liver enzymes is observed after applying Wnt inhibitors in the mouse model. This was also histologically observed by reduced liver inflammation and fibrosis. These results imply that by lowering underlying inflammatory processes, addressing Wnt signalling may be a useful treatment approach for cholestatic liver disorders (30).

In contrast to the changed Inversin expression, DVL-1 expression remains relatively stable throughout the observed developmental stages, suggesting a different regulatory pathway or a compensatory mechanism in response to the *Dab1* mutation. Although our results show no significant difference in Dvl-1 expression in wild-type and *yot* mice, it is still important to mention the importance of Dvl-1 for our understanding of hepatocellular cancer (HCC).

There is a close association between the DVL proteins, DVL-1 in particular, and HCC due to their integral role in the Wnt pathway. The major role in HCC development gives the potential of using DVL-1 as a prognostic indicator (23). Superpotent cancer stem cells (CSC) of HCC cancer have been proven to have increased expression of DVL-1. This is due to the protein's role in cellular regulation, which preserves the stemness and tumorigenic capacity of the CSCs. This can be vital in furthering our understanding of HCC, its prognostic factors and therapeutic targets (31).

The primary limitation of our study is its observational nature. Since our samples consist of archived embryonic mice liver tissue that was paraffin-embedded and formalin-fixed, we were unable to perform quantitative protein expression analyses such as flow cytometry or Western blotting. Despite this limitation, our findings are valuable as they illustrate the changes in Inversin and DVL-1 immunoexpression in the liver due to the inactivation of the *Dab1* gene.

This study provides a foundation for future research to understand how genetic mutations disrupt normal liver development, potentially leading to targeted therapeutic interventions for congenital anomalies and diseases.

6. CONCLUSION

1. By embryonic day 13.5 (E13.5), the liver has reached its definitive embryonic structure. This stage is marked by peak hematopoietic activity, with a high density of hematopoietic cells. Hepatoblasts are densely packed in the peripheral regions of the liver, exhibiting minimal intercellular communication. Megakaryocytes are abundant, and erythroblastic islands, consisting of central F4/80-positive macrophages surrounded by mature erythroblasts, are widely distributed.

2. At embryonic day 15.5 (E15.5), the liver maintains a structure similar to that observed at E13.5, but hematopoietic activity declines. Red blood cells mature, expelling their nuclei and resulting in various erythrocyte sizes. Megakaryocytes remain prevalent, and key vascular structures such as the *ductus venosus*, caudal *vena cava*, and portal vein are visible.

3. Hematoxylin and Eosin (H&E) staining revealed no significant morphological differences between the livers of control specimens and those of *yot* mutants. This indicates that the liver's overall structure and cellular composition remain consistent across these samples during the observed developmental stages.

4. Inversin plays a crucial role in modulating Wnt signaling pathways, essential for cellular processes and tissue development.This study investigated the expression of Inversin (Invs) during liver development in wild-type and *yot* ($Dab1^{-/-}$) mutant mice, revealing distinct patterns in Invs-positive cells.

5. In wild-type mice, there was a progressive increase in the percentage of Invs-positive cells from gestation day E13.5 to E15.5. In contrast, *yot* mice exhibited a decrease in the percentage of Invs-positive cells over the same developmental period. Furthermore, analysis of the area percentage of Invs-positive cells showed significantly higher expression in *yot* mice at E13.5 compared to wild-type mice. However, by E15.5, this expression significantly declined in *yot* mice relative to wild-type counterparts.

6. The increase in Invs expression at E13.5 suggests a potential role in early liver development specific to *yot* mutants. The subsequent decline by E15.5 may indicate regulatory mechanisms or developmental transitions affected by the *Dab1* mutation.

7. The fluctuating expression of Invs in *yotari* mice highlights its potential involvement in liver development and suggests further exploration into its specific functions and interactions within the Wnt signaling network. Understanding these dynamics could

provide insights into the mechanisms underlying liver developmental disorders associated with Dab1 mutations and potential avenues for therapeutic interventions.

8. Analysis of Dvl-1 area percentage between wild-type and *yot* (*Dab1-/-*) mutant mice revealed consistent staining patterns across both phenotypes at observed time points. Generally, a higher area percentage of positive cells for Dvl-1 was observed in wild-type mice compared to *yot* mice. Over the developmental period from E13.5 to E15.5, we observed a decreasing trend in the percentage of Dvl-1 positive cells in wild-type mice, whereas *yot* mice showed an increasing trend.

9. A stable DVL-1 expression throughout the observed stages implies a distinct regulatory pathway or compensatory mechanism in response to the genetic mutation.

10. The co-expression of Inversin and Dvl-1 in the cytoplasm of maturing hepatocytes was noted in both *yot* and wild-type mice, highlighting their potential interaction in liver development processes.

11. These findings underscore the regulatory role of the Dab1 gene in modulating Invs expression during critical stages of liver development. The observed differences highlight potential disruptions in Wnt signaling pathways in Yot mice, suggesting implications for understanding congenital liver anomalies and diseases associated with dysregulated Invs expression. Further research into the mechanistic insights of Invs modulation could pave the way for targeted therapeutic strategies aimed at mitigating liver developmental disorders.

7. REFERENCES

1. Vernon H, Wehrle CJ, Alia VSK, Kasi A. Anatomy, abdomen and pelvis: Liver. StatPearls [Internet].2022 Nov 26 [cited 2024 May 11]; Available from: https://www.ncbi.nlm.nih.gov/books/NBK500014/

2. Trefts E, Gannon M, Wasserman DH. The liver. Curr Biol. 2017;27:R1147-R1151.

3. Garg S, Kumar KH, Sahni D, Yadav TD, Aggarwal A, Gupta T. Anatomy of the hepatic arteries and their extrahepatic branches in the human liver: A cadaveric study. Ann Anat. 2020;227:151409.

4. Treuting PM, Dintzis SM, Montine KS. comparative anatomy and histology a mouse, rat, and human atlas Second Edition. 2018. p. 191-211

5. Paštar V, Lozić M, Kelam N, Filipović N, Bernard B, Katsuyama Y, et al. Connexin expression is altered in liver development of yotari (Dab1 -/-) mice. Int J Mol Sci. 2021;22:10712.

6. Zorn AM. Liver development. 2008 Oct 31. In: StemBook [Internet]. Cambridge (MA): Harvard Stem Cell Institute; 2008–. Available from https://www.ncbi.nlm.nih.gov/books/NBK27068/

7. Yoneshima H, Nagata E, Matsumoto M, Yamada M, Nakajima K, Miyata T, et al. Neuroscience research a novel neurological mutant mouse, yotari, which exhibits reeler-like phenotype but expresses CR-50 antigen/Reelin. Neurosci Res. 1997;29:217-23.

8. Arimitsu N, Mizukami Y, Shimizu J, Takai K, Suzuki T, Suzuki N. Defective Reelin/Dab1 signaling pathways associated with disturbed hippocampus development of homozygous yotari mice. Mol Cell Neurosci. 2021;112:103614.

9. Sheldon M, Rice DS, D'Arcangelo G, Yoneshima H, Nakajima K, Mikoshiba K, et al. Scrambler and yotari disrupt the disabled gene and produce a reeler-like phenotype in mice. Nature. 1997;389:730-3.

10. Lodish H, Berk A, Kaiser CA, Krieger M, Bretscher A, Ploegh H, Amon A, Martin KC. *The Cell: A Molecular Approach*. 8th ed. New York (NY): W.H. Freeman and Company; 2021.

11. Sharma M, Pruitt K. Wnt pathway: An integral hub for developmental and oncogenic signaling networks. Int J Mol Sci. 2020;1:1–24.

12.   Qin K, Yu M, Fan J, Wang H, Zhao P, Zhao G, et al. Canonical and noncanonical Wnt signaling: Multilayered mediators, signaling mechanisms and major signaling crosstalk. Genes Dis. 2024;11:103–34.

13.   Dlugosz P, Teufl M, Schwab M, Kohl KE, Nimpf J. Disabled 1 is part of a signaling pathway activated by epidermal growth factor receptor. Int J Mol Sci. 2021;22:1745.

14.   Perutina I, Kelam N, Maglica M, Racetin A, Ogorevc M, Filipović N, et al. Disturbances in switching between canonical and non-canonical Wnt signaling characterize developing and postnatal kidneys of Dab1−/− (yotari) Mice. Biomedicines. 2023;11:1321.

15.   Lee GH, D'Arcangelo G. New Insights into Reelin-Mediated Signaling Pathways. Front Cell Neurosci. 2016;10:122.

16.   Simons M, Gloy J, Ganner A, Bullerkotte A, Bashkurov M, Krönig C, et al. Inversin, the gene product mutated in nephronophthisis type II, functions as a molecular switch between Wnt signaling pathways. Nat Genet. 2005;37:537–43.

17.   Mochizuki T, Saijoh Y, Tsuchiya K, Shirayoshi Y, Takai S, Taya C, Yonekawa H, Yamada K, Nihei H, Nakatsuji N, Overbeek PA, Hamada H, Yokoyama T. Cloning of inv, a gene that controls left/right asymmetry and kidney development. Nature. 1998;395:177-81.

18.   Lienkamp S, Ganner A, Walz G. Inversin, Wnt signaling and primary cilia. Differentiation. 2012;83:S49–55.

19.   Lienkamp S, Ganner A, Boehlke C, Schmidt T, Arnold SJ, Schäfer T, et al. Inversin relays Frizzled-8 signals to promote proximal pronephros development. Proc Natl Acad Sci U S A. 2010;107:20388–93.

20.   Nü J, Bacallao RL, Phillips CL. Inversin forms a complex with catenins and N-cadherin in polarized epithelial cells. Mol Biol Cell. 2002;13:3096–106.

21. Sharma M, Castro-Piedras I, Simmons GE, Pruitt K. Dishevelled: A masterful conductor of complex Wnt signals. Cell Signal. 2018:47:52–64.

22.   Xu T, Pan L, Li L, Hu S, Zhou H, Yang C, et al. MicroRNA-708 modulates hepatic stellate cells activation and enhances extracellular matrix accumulation via direct targeting TMEM88. J Cell Mol Med. 2020;24:7127–40.

23. Mei J, Yang X, Xia D, Zhou W, Gu D, Wang H, et al. Systematic summarization of the expression profiles and prognostic roles of the dishevelled gene family in hepatocellular carcinoma. Mol Genet Genomic Med. 2020;8:e1384.

24. Solic I, Racetin A, Filipovic N, Mardesic S, Bocina I, Galesic-Ljubanovic D, et al. Expression pattern of α-tubulin, inversin and its target dishevelled-1 and morphology of primary cilia in normal human kidney development and diseases. Int J Mol Sci. 2021;22:3500.

25. Arimitsu N, Mizukami Y, Shimizu J, Takai K, Suzuki T, Suzuki N. Defective Reelin/Dab1 signaling pathways associated with disturbed hippocampus development of homozygous yotari mice. Mol Cell Neurosci. 2021;112:103614.

26. Wu J, Cai Y, Wu X, Ying Y, Tai Y, He M. Transcardiac Perfusion of the Mouse for Brain Tissue Dissection and Fixation. Bio Protoc. 2021;11:e3988.

27. Wang H, Zaiser F, Eckert P, Ruf J, Kayser N, Veenstra AC, et al. Inversin (NPHP2) and Vangl2 are required for normal zebrafish cloaca formation. Biochem Biophys Res Commun . 2023;673:9–15.

28. Mazziotti MV, Willis LK, Heuckeroth RO, LaRegina MC, Swanson PE, Overbeek PA, Perlmutter DH. Anomalous development of the hepatobiliary system in the Inv mouse. Hepatology. 1999;30:372-8.

29. Preziosi ME, Singh S, Valore E V., Jung G, Popovic B, Poddar M, et al. Mice lacking liver-specific β-catenin develop steatohepatitis and fibrosis after iron overload. J Hepatol. 2017;67:360–9.

30. Ayers M, Kosar K, Xue Y, Goel C, Carson M, Lee E, et al. Inhibiting Wnt Signaling Reduces Cholestatic Injury by Disrupting the Inflammatory Axis. CMGH. 2023;16:895–921.

31. Liao WY, Hsu CC, Chan TS, Yen CJ, Chen WY, Pan HW, et al. Dishevelled 1-regulated superpotent cancer stem cells Mediate Wnt heterogeneity and tumor Progression in hepatocellular carcinoma. Stem Cell Reports. 2020;14:462–77.

8. SUMMARY

Objectives: Invs and DVL-1 expression patterns in the liver of *yot* (*Dab1*-/-) mice are the focus of this study, which attempts to clarify their possible roles in the pathophysiology of hepatic abnormalities linked to the *Dab1* loss. This study aims to advance knowledge of the molecular processes that underlie the emergence of hepatic dysfunction in the context of *Dab1* disruption, elucidating possible ramifications for hepatic physiology and associated treatment approaches.

Materials and methods: Homozygous $Dab1^{-/-}$ *yot* mutant mice, who have an autosomal recessive mutation of the *Dab1* gene, and C57BL/6N wild-type mice were used. The gravid mice were sacrificed on embryonic days 13.5 and 15.5 in order to obtain their embryos and their tissue was fixed and stained using immunofluorescence antibodies for Inversin and Dvl-1 proteins. The groups were analysed using a two-way ANOVA test.

Results: The findings revealed distinct positive expression patterns, differing in intensity, distribution, and quantity. In wild-type mice, the percentage of Invs-positive cells increased from gestation day E13.5 to E15.5, while it decreased in *yot* mice over the same period. Specifically, at E13.5, Invs expression was significantly higher in *yot* mice compared to wild-type mice but dropped significantly by E15.5. In contrast, Dvl-1 expression patterns showed minimal variation between the two phenotypes at both time points, with generally higher percentages of Dvl-1 positive cells in wild-type mice. Over the period from E13.5 to E15.5, wild-type mice exhibited a decreasing trend in Dvl-1 positive cells, whereas *yo*t mice showed an increasing trend.

Conclusion: Hematoxylin and Eosin (H&E) staining indicates no significant liver morphology differences between control and yot mutants, while Inversin expression increases in wild-types and decreases in yot mutants from E13.5 to E15.5, with yot mutants showing higher Invs expression at E13.5 but a significant decline by E15.5. Conversely, Dvl-1 positive cells decrease in wild-types and increase in yot mutants, with Invs and Dvl-1 co-expressed in hepatocytes, suggesting interaction in liver development and potential compensatory mechanisms.

9. CROATIAN SUMMARY

Naslov: EKSPRESIJA INVERSINA I DVL-1 U JETRI *YOTARI* (*DAB1*^{-/-}) I DIVLJEG TIPA MIŠA

Ciljevi: Obrasci ekspresije Invs i Dvl-1 u jetri yot (Dab1-/-) miševa fokus su ove studije, koja pokušava razjasniti njihove moguće uloge u patofiziologiji jetrenih abnormalnosti povezanih s gubitkom Dab1. Ova studija ima cilj unaprijediti znanje o molekularnim procesima koji su u osnovi pojave jetrene disfunkcije u kontekstu poremećaja Dab1, razjašnjavajući moguće posljedice za jetrenu fiziologiju i povezane pristupe liječenju.

Materijali I metode: Korišteni su homozigotni miševi Dab1$-/-$ yot mutanti, koji imaju autosomno recesivnu mutaciju gena Dab1, i C57BL/6N miševi divljeg tipa. Gravidni miševi žrtvovani su embrionalnih dana 13,5 i 15,5 kako bi se dobili njihovi embriji, a njihovo tkivo je fiksirano i obojeno upotrebom imunofluorescentnih antitijela za proteine Inversin i Dvl-1. Skupine su analizirane pomoću dvosmjernog ANOVA testa.

Rezultati: Nalazi su otkrili različite pozitivne obrasce ekspresije, koji se razlikuju po intenzitetu, distribuciji i količini. Kod miševa divljeg tipa, postotak Invs-pozitivnih stanica porastao je od dana gestacije E13.5 do E15.5, dok se smanjio kod Yot miševa tijekom istog razdoblja. Konkretno, na E13.5, ekspresija Invs bila je značajno viša kod Yot miševa u usporedbi s miševima divljeg tipa, ali je značajno pala za E15.5. Nasuprot tome, obrasci ekspresije Dvl-1 pokazali su minimalnu varijaciju između dva fenotipa u obje vremenske točke, s općenito višim postocima Dvl-1 pozitivnih stanica u miševa divljeg tipa. Tijekom razdoblja od E13.5 do E15.5, miševi divljeg tipa pokazali su trend smanjenja Dvl-1 pozitivnih stanica, dok su miševi yot pokazali trend povećanja.

Zaključci: Bojanje hematoksilinom i eozinom (H&E) ukazuje da nema značajnih razlika u morfologiji jetre između kontrolnih i yot mutanata, dok se ekspresija Inversina povećava u divljim tipovima i smanjuje u yot mutantima s E13.5 na E15.5, pri čemu yot mutanti pokazuju veću ekspresiju Invs na E13 .5 ali značajan pad za E15.5. Nasuprot tome, Dvl-1 pozitivnih stanica smanjuje se u divljim tipovima i povećava u yot mutantima, s Invs i Dvl-1 ko-eksprimiranim u hepatocitima, što ukazuje na interakciju u razvoju jetre i potencijalne kompenzacijske mehanizme.